Metal−Protein Interactions: Structure Information from Ni^{2+}-Induced Pseudocontact Shifts in a Native Nonmetalloprotein†

Malene Ringkjøbing Jensen and Jens J. Led*

Department of Chemistry, University of Copenhagen, Universitetsparken 5, DK-2100 Copenhagen Ø, Denmark
Received March 6, 2006; Revised Manuscript Received May 30, 2006

ABSTRACT: Information about the structure of a native nonmetalloprotein was obtained from the pseudocontact shifts induced by a paramagnetic metal ion bound to the protein. The approach exploits the presence of metal binding sites on the surface of the protein. Using *Escherichia coli* thioredoxin as a model protein, we show that potential binding sites can be identified using the Cu^{2+} ion, and that pseudocontact shifts induced by a Ni^{2+} ion bound to one of these sites can provide valuable long-range structure information about the protein.

Paramagnetic metal ions are important tools in the studies of the structure and function of proteins and nucleic acids. In particular, the pseudocontact shifts of the protein nuclei can provide valuable long-range structure information. These shifts are caused by the dipolar interactions between the nuclei and the unpaired electrons of the metal ion and can be observed in the nuclear magnetic resonance (NMR)[1] spectra of the proteins. This long-range structure information is particularly valuable in the determination of the solution structures of nucleic acids and proteins, where the conventional NMR method fails because of an insufficient number of observable nuclear Overhauser enhancements (NOEs), as demonstrated for paramagnetic metallo−DNA complexes (*1*−*3*), native paramagnetic metalloproteins (*4*−*9*), and nonmetalloproteins with a tag-bound paramagnetic metal ion (*10*−*15*).

Here, we show that paramagnetic metal ions can be used in the structure determination of a native nonmetalloprotein, even without the use of metal binding tags. The applicability of this approach is suggested by the fact that many nonmetalloproteins bind metal ions, in particular on the surface of the molecules. These metal ions may play an important role for the stabilization or crystallization of the proteins, or they may function as cofactors. Here, we demonstrate the potential applicability of the pseudocontact shifts induced by a surface-bound metal ion, to obtain long-range structure information about a protein in solution. *Escherichia coli* (*E. coli*) thioredoxin (Trx) was used as a model protein, while Ni^{2+} was used as the paramagnetic metal ion.

† This work was financially supported by the Danish Natural Science Research Council, J. Nos. 9400351, 51-00211, and 21-04-0519, Carlsbergfondet, J. No. 1624/40, Novo Nordisk Fonden, J. No. 2003-11-28, and Villum Kann Rasmussen Fonden, J. No. 8.12.2003.

* Corresponding author. Jens J. Led, Department of Chemistry, University of Copenhagen, Universitetsparken 5, DK-2100 Copenhagen Ø, Denmark, Phone, +45 35320302; fax, +45 35320322; e-mail, led@kiku.dk.

[1] Abbreviations*:* NMR, nuclear magnetic resonance; NOE, nuclear Overhauser enhancement; *E. coli*, *Escherichia coli*; Trx, thioredoxin; rmsd, root-mean-square deviation.

MATERIALS AND METHODS

NMR Samples. Cloning, expression, and purification of *E. coli* Trx were performed as described previously (*16*). The protein was dissolved in 90% H_2O/10% D_2O with 50 mM sodium choride. The protein concentration was either 0.5 mM or 1.0 mM. The oxidized form of the protein was obtained by adding 5 μL of 50 mM H_2O_2 to each NMR sample (1.0 mM, 500 μL). Coordination of the applied metal ions was achieved by adding the appropriate amounts of $NiCl_2 \cdot 6H_2O$, $CuCl_2 \cdot 2H_2O$, $ZnCl_2$, or $CdCl_2 \cdot 2.5H_2O$ to the protein samples. After the addition of the metal ions, the pH was adjusted to 7.0. The samples were sealed under nitrogen.

NMR Experiments. The NMR experiments were carried out at 298 K and a ^1H frequency of 500 MHz, using a Varian Unity Inova 500 spectrometer equipped with a cold probe. The ^1H-^{15}N HSQC spectra were collected with either 2048 or 4096 t_2 data points and 150 t_1 slices. The sweep width was 10 and 2.2 kHz in the ^1H and ^{15}N dimension, respectively. The TOCSY spectra consisted of 2048 t_2 data points and 512 t_1 slices. The sweep width was 10 kHz in both dimensions. In all experiments, the ^1H carrier was placed on the residual HDO resonance.

RESULTS AND DISCUSSION

Locating Potential Binding Sites in Thioredoxin. Potential metal binding sites on the surface of a protein can be located using the paramagnetic Cu^{2+} ion. Thus, if Cu^{2+} binds with an appreciable affinity to the protein surface, the signals of nuclei spatially close to the binding site will undergo substantial line broadening due to the long electron relaxation time of Cu^{2+} and the dipole−dipole interaction between the nuclei and the unpaired electron of Cu^{2+}. This approach was used here for locating a binding site on the surface of Trx. Upon addition of an equivalent amount of Cu^{2+} to a sample of metal-free Trx, several amide signals in the ^1H-^{15}N HSQC spectrum of the Cu^{2+} containing protein are broadened beyond detection due to the interaction

10.1021/bi0604431 CCC: $33.50
Published on Web 07/01/2006

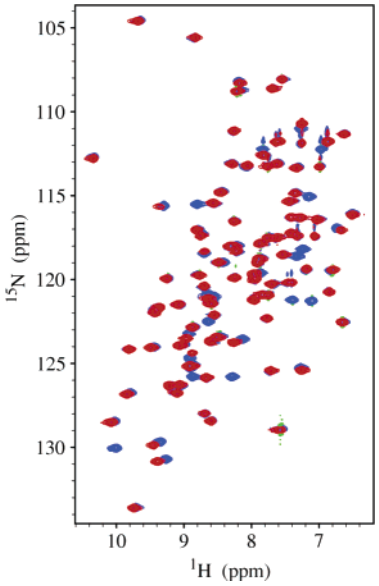

FIGURE 1: Superposition of the ^{1}H-^{15}N HSQC spectrum of a 1.0 mM sample of metal-free Trx at pH 7.0 (blue peaks) and the ^{1}H-^{15}N HSQC spectrum of a 0.5 mM sample of Trx containing an equivalent amount of the paramagnetic Cu^{2+} ion (red peaks).

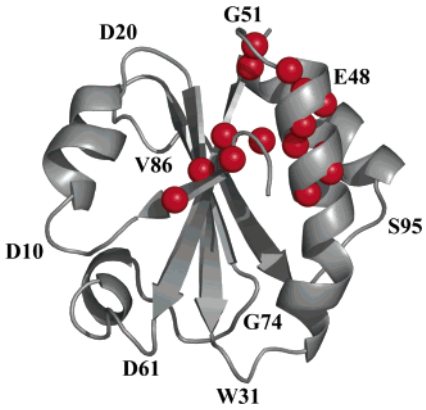

FIGURE 2: Ribbon model of the solution structure of Trx. The red spheres indicate the amide protons, the signals of which disappear in the ^{1}H-^{15}N HSQC spectrum upon addition of the paramagnetic Cu^{2+} ion to a sample of Trx.

with the unpaired electron (see Figure 1). As shown in Figure 2, all protons with unobservable signals are spatially close to the N-terminus, indicating the presence of a binding site near the N-terminus of Trx. This binding site is also found in the crystal structure of Trx (*17*). Thus, Trx crystallized in the presence of cupric acetate reveals a Cu^{2+} ion bound to the N-terminal nitrogen atom of S1, the amide nitrogen of residue D2, and the side chain atom OD1 of residue D2.

As seen in Figure 1, the amide protons that are observed in the HSQC spectrum of the Cu^{2+}-containing protein only give rise to single signals, indicating fast exchange between the metal-free and the metal-bound forms of the protein. Moreover, some of the signals are shifted relative to those of the metal-free sample, indicating significant Cu^{2+}-induced pseudocontact shifts. To determine these shifts, the fraction of metal-bound protein must be estimated. Although this can be done on the basis of the longitudinal paramagnetic relaxation of the ^{1}H nuclei (*18*), the reduced number of observable signals makes Cu^{2+} less suitable here for gaining information about the protein structure. Yet, the Cu^{2+}–protein interaction is valuable for identifying potential metal binding sites.

The Interaction between Ni^{2+} and Thioredoxin. The paramagnetic Ni^{2+} ion binds at the N-terminus of Trx in a similar way as the Cu^{2+} ion, and with an apparent dissociation constant of 607 μM (*16*). However, unlike the Cu^{2+} ion, the exchange of the Ni^{2+} ion is slow ($k_{ex} = 13.5\ s^{-1}$ for a 1.0 mM sample of Trx at pH 7.0 with 1.0 mM Ni^{2+}), leading to separate NMR signals from the metal-free and the metal-bound form for several of the amide groups (see Figure 3). Furthermore, the short electron relaxation time of the Ni^{2+} ion allows the observation of almost all the proton signals of the metal-bound form. The chemical shift, δ, of a nucleus in the metal-bound form is given by

$$\delta = \delta_{dia} + \delta_{struct} + \delta_{charge} + \delta_{pcs} + \delta_{con} \qquad (1)$$

where δ_{dia} is the chemical shift in the metal-free protein, δ_{struct} and δ_{charge} are the chemical shift contributions from the changes in structure and charge at the N-terminus caused by the Ni^{2+} binding, δ_{pcs} is the pseudocontact shift, and δ_{con} is the contact shift caused by the scalar coupling between the nucleus and the unpaired electrons. Here, the contact shift is negligible, since only nuclei outside the first coordination sphere are considered.

The changes in the overall structure of the protein upon binding of the metal ion are only minor, as indicated by the small difference between the crystal (metal-bound) structure (*17*) (PDB: 2TRX) and the solution (metal-free) structure (*19*) (PDB: 1XOA) of Trx. Furthermore, the ^{1}H chemical shifts of the nuclei of the metal-bound form are unaffected by the change in the charge at the N-terminus upon binding of Ni^{2+}. Thus, addition (equivalent amounts and excess) of the diamagnetic Zn^{2+} and Cd^{2+} ions to the metal-free protein solution has no significant effect on the HSQC spectrum. This could reflect a substantially smaller binding affinity of Zn^{2+} and Cd^{2+} as compared to Cu^{2+} and Ni^{2+}. However, also protonation of the N-terminus of Trx leaves the chemical shifts of the ^{1}H nuclei beyond residue S1 unaffected (*20*). Therefore, all taken together, the ^{1}H chemical shift changes shown in Figure 3 must be dominated by Ni^{2+}-induced pseudocontact shifts. This is further supported by the observation that the corresponding Cu^{2+}- and Ni^{2+}-induced shifts for several residues (Figure 1 and Figure 3, respectively) have opposite sign. These opposite shifts are incompatible with both charge- and structure-induced shifts and can only be explained by differences in the size and/or orientation of the magnetic susceptibility tensor of the Ni^{2+} and the Cu^{2+} ion. A similar observation has been made for the blue copper protein azurin, where the Cu^{2+}-induced pseudocontact shifts have the opposite sign of the corresponding shifts in the Ni^{2+}-substituted protein (*21*).

It should be noted that accurate pseudocontact shifts are obtained only if the slow exchange condition applies; that is, the rate of exchange between the metal-free and the Ni^{2+}-bound protein is small compared to the chemical shift difference between the two forms. For the rate constant, $k_{ex} = 13.5\ s^{-1}$, estimated for this exchange process in a 1.0 mM sample of Trx at pH 7.0 with 1.0 mM Ni^{2+} (*16*), the slow exchange condition is fulfilled even for very small pseudocontact shifts ($\delta_{pcs} = 0.03$ ppm).

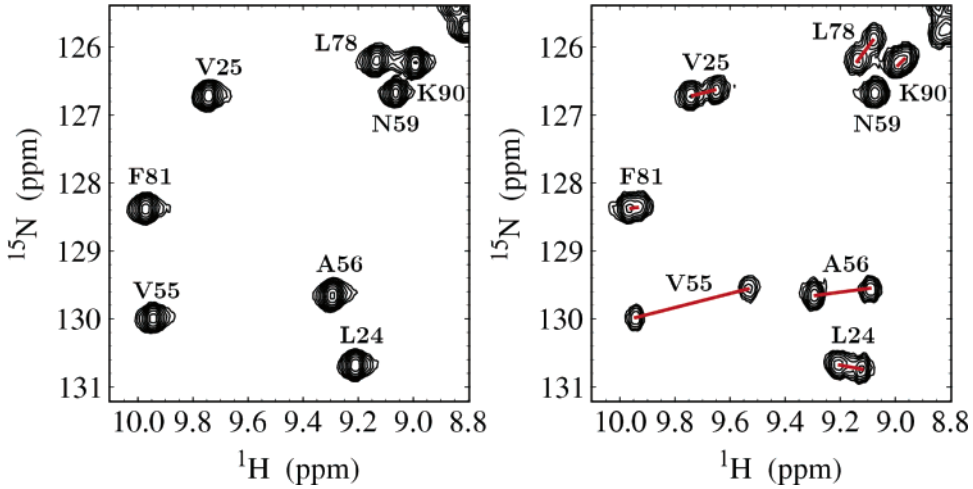

FIGURE 3: Part of the ^{1}H-^{15}N HSQC spectrum of a 1.0 mM sample of Trx at pH 7.0 without (left) and with (right) 1.0 mM Ni^{2+}. The labels indicate the assignments of the different amide groups. Additional signals, corresponding to the metal-bound form of the protein, appear in the spectrum of the protein sample containing the paramagnetic Ni^{2+} ion.

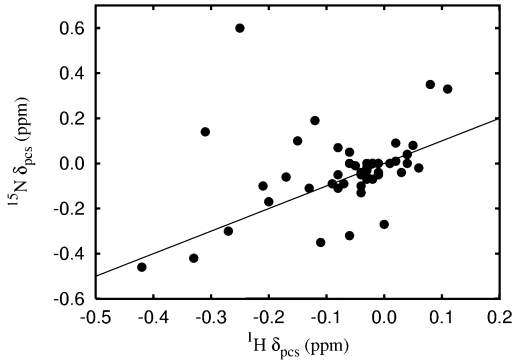

FIGURE 4: Comparison of the experimental Ni^{2+}-induced pseudocontact shifts of the amide protons and the amide ^{15}N nuclei in Trx.

The pseudocontact shift, δ_{pcs}, is given by (*22*)

$$\delta_{pcs} = \frac{1}{12\pi r^3}\left[\Delta\chi_{ax}(3\cos^2\theta - 1) + \frac{3}{2}\Delta\chi_{rh}\sin^2\theta\cos(2\phi)\right] \quad (2)$$

Here, $\Delta\chi_{ax}$ and $\Delta\chi_{eq}$ are the axial and the rhombic part of the magnetic susceptibility tensor, respectively, and r, θ, and ϕ are the spherical coordinates of the nucleus in the principal coordinate system of the magnetic susceptibility tensor.

Experimental ^{1}H and ^{15}N Pseudocontact Shifts. According to eq 2, the pseudocontact shifts are independent of the specific type of nucleus. Therefore, comparable pseudocontact shifts are expected for the ^{1}H and ^{15}N nuclei of the same amide group. Yet, the observed Ni^{2+}-induced pseudocontact shifts are rather different for the two nuclei for a number of residues in Trx, as shown by the comparison in Figure 4. Similar differences in ^{1}H and ^{15}N pseudocontact shifts observed previously in iron−sulfur proteins and blue copper proteins (*23*−*27*) were ascribed to minor differences in structure and charge between the paramagnetic and diamagnetic protein that cause (minor) changes of the ^{15}N chemical shifts and not the ^{1}H chemical shifts. The latter conclusion is supported by the fact that the ^{15}N chemical shifts are in general more sensitive to small changes in the structure and charge than are the ^{1}H chemical shifts (*28*, *29*). Similar minor changes in the ^{15}N chemical shifts upon Ni^{2+} binding could explain the differences between the ^{1}H and ^{15}N pseudocontact shifts shown in Figure 4. Furthermore, if delocalization of the unpaired electron spin onto the $2p_z$ orbitals of the ^{15}N nuclei is present (*30*), an additional contribution to the ^{15}N pseudocontact shifts is expected.

Here, only the ^{1}H pseudocontact shifts were used in the structural refinement in order to minimize errors caused by the δ_{struct} and δ_{charge} contributions. Experimentally, the Ni^{2+}-induced ^{1}H pseudocontact shifts were obtained from either the HSQC spectrum (amide protons) or the TOCSY spectrum (α- and some β-protons) of Trx containing an equivalent amount of Ni^{2+}. The assignment of the metal-bound form was obtained by identifying the spin systems of the metal-bound signals in the TOCSY spectrum. Nonzero pseudocontact shifts were obtained for the nuclei between 9 and 25 Å from the N-terminus of the protein, the size of the pseudocontact shifts being dependent on the position of the nuclei within the principal coordinate system of the χ-tensor.

Contributions from other Metal Binding Sites on the Protein Surface. Four additional metal binding sites, that is, the side chain carboxylate groups of the residues D10, D20, D47, and E85, are present on the surface of Trx. These are weak Ni^{2+} binding sites (D10, 2.4 mM; D20, 4.6 mM; D47, 13.6 mM; and E85, 20 mM) with fast exchange of the Ni^{2+} ion (*16*) and no Ni^{2+}-induced pseudocontact shifts. Thus, for instance, no pseudocontact shifts are observed for T8, D9, D10, S11, and F12 that all are close to the D10 site (see Supporting Information).

The Reliability and Applicability of the Obtained Ni^{2+}-Induced ^{1}H Pseudocontact Shifts. Primarily, the agreement of the obtained ^{1}H pseudocontact shifts with the solution structure of Trx was investigated by including the pseudocontact shifts as restraints in a structural refinement, using the Xplor-NIH program (*31*) and the module PARArestraints (*32*). The structure refinement was carried out as described previously (*25*). An initial structure of the metal−protein complex was obtained from the solution structure of *E. coli* Trx (*19*) by including a Ni^{2+} ion at the N-terminal end of the protein. The orientation and the size of the magnetic susceptibility tensor were obtained during the refinement protocol, where NOEs, dihedral angles, and the experimental pseudocontact shifts were included as restraints. The initial

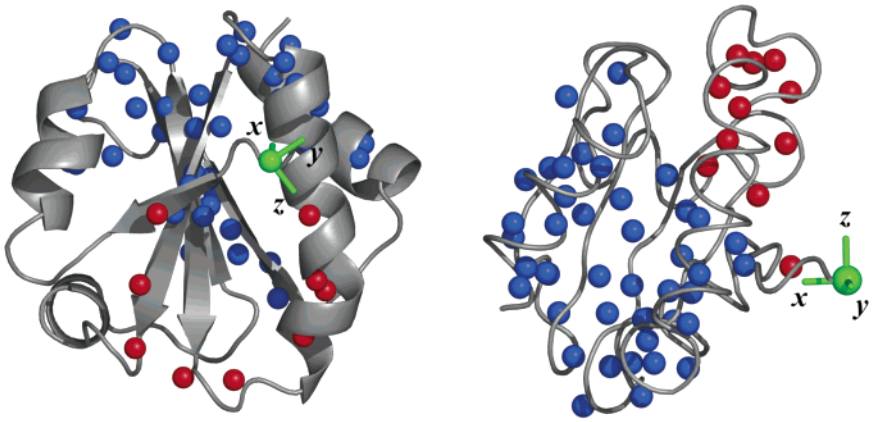

FIGURE 5: The orientation of the magnetic susceptibility tensor within the molecular frame of the refined solution structure of Trx with the experimental pseudocontact shifts. The green spheres indicate the paramagnetic Ni^{2+} ion. Amide protons with positive experimental pseudocontact shifts are shown in red, while amide protons with negative pseudocontact shifts are shown in blue. Left panel: the view of the molecule is identical to that in Figure 2. Right panel: different view of the molecule showing the agreement between the orientation of the magnetic susceptibility tensor and the distribution of positive and negative pseudocontact shifts.

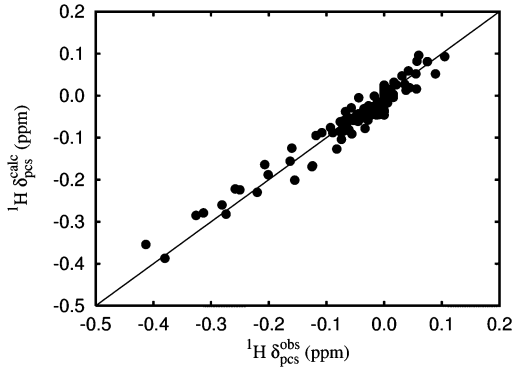

FIGURE 6: Comparison of the observed and calculated ^1H pseudocontact shifts. The calculated pseudocontact shifts were obtained using the module PARArestraints available for Xplor-NIH (see text).

parameters chosen for the axial and the rhombic part of the susceptibility tensor were $\Delta\chi_{ax} = 2.3 \times 10^{-32}$ m^3 and $\Delta\chi_{rh} = 0.0 \times 10^{-32}$ m^3, and 50 structures were calculated for each of the 10 iterations of the tensor parameters. A relatively small force constant of 7 kcal mol^{-1} ppm^{-2} was used for the paramagnetic restraints in order to investigate the agreement between the protein structure and the observed pseudocontact shifts. A tolerance of 0.05 ppm was used for all the experimental pseudocontact shifts. During the refinement protocol, the tensor parameters converge to $\Delta\chi_{ax} = 1.29 \times 10^{-32}$ m^3 and $\Delta\chi_{rh} = -0.59 \times 10^{-32}$ m^3.

Figure 5 shows the distribution of the pseudocontact shifts in the structure of Trx as well as the obtained orientation of the magnetic susceptibility tensor within the molecular frame. As it appears from the figure, the majority of the experimental pseudocontact shifts are negative, in agreement with the obtained orientation of the magnetic susceptibility tensor. As shown in Figure 6, the experimental pseudocontact shifts are in good agreement with the shifts calculated from the protein structure and the susceptibility tensor. Further evaluation of the agreement between the experimental and the calculated pseudocontact shifts was made by omitting a small portion (15 %) of the experimental pseudocontact shifts, and back-calculating the shifts from the subsequent analysis. The omitted pseudocontact shifts were randomly selected among the 137 observables, and the procedure was repeated 10 times. The agreement between the omitted pseudocontact shifts and the back-calculated shifts was evaluated through the *Q*-parameter (*33*). An average *Q*-parameter of 31 ± 3% was obtained.

The structure of Trx is slightly improved upon refinement with the experimental pseudocontact shifts. Thus, the backbone root-mean-square deviation (rmsd) of the 10 structures with lowest total energy is 0.41 Å before the refinement and 0.34 Å after the refinement. However, the NMR solution structure of Trx is based on a total of 2700 NOEs, which makes it difficult to improve the structure further, and thereby to evaluate the significance of the pseudocontact shifts.

Therefore, the usefulness of the experimental pseudocontact shift as a replacement for the long-range NOE was examined by using a reduced set of NOEs in the structure calculation. The pseudocontact shifts are expected to be most important in regions where the NOEs are difficult to obtain, as for instance in flexible regions of the molecule or in crowded spectral regions. However, the two kinds of restraints are rather different in nature, the pseudocontact shift being genuinely long-range in space, while the NOEs are short-range in space and only long-range in the primary structure. Therefore, it is not immediately apparent to what extent such a replacement is possible or useful. To investigate this, an increasing number of long-range NOEs were randomly removed from the structure calculations, while the experimental pseudocontact shifts, the short-range NOEs, and the dihedral angles were retained as restraints. The total number of long-range NOEs in Trx is 810. The calculations were carried out using the following numbers of long-range NOEs: 600, 400, 200, 100, 50, and 25. Within each group, the calculation was repeated five times with different randomly selected NOEs, and 50 structures were calculated each time. The tensor parameters were kept fixed at $\Delta\chi_{ax} = 1.29 \times 10^{-32}$ m^3 and $\Delta\chi_{rh} = -0.59 \times 10^{-32}$ m^3 (see above), and a force constant of 100 kcal mol^{-1} ppm^{-2} was used for the paramagnetic restraints. For comparison, similar calculations were performed with the experimental pseudocontact shifts excluded. The calculations show that the paramagnetic restraints improve both the precision of the structure, defined as the backbone rmsd of the ensemble of the 10 structures with lowest energy, and the accuracy defined as the rmsd between the lowest energy structure and the protein solution

structure (PDB: 1XOA). Thus, for example, if only 50 out of the 810 long-range NOEs are included, the precision is improved from 0.95 to 0.89 Å when the experimental pseudocontact shifts are included as restraints, while the accuracy is improved from 2.66 to 2.22 Å. If the number of long-range NOEs are reduced to only 25, the precision is improved from 1.75 to 1.54 Å, while the accuracy is improved from 4.96 to 4.02 Å. It should be mentioned that only a small improvement is seen, if the number of included long-range NOEs exceeds 200. Furthermore, the Ramachandran statistics are very similar with and without the paramagnetic restraints included. Nevertheless, the study clearly shows that the experimental pseudocontact shifts contain a significant amount of structure information.

CONCLUSION

In conclusion, it is demonstrated that pseudocontact shifts induced by the paramagnetic Ni^{2+} ion bound to the protein surface can provide valuable structure information, even if the metal binding affinity is modest. Also, it is shown that potential metal binding sites on the surface of a native nonmetalloprotein can be identified using the paramagnetic Cu^{2+} ion as a probe. In general, the approach requires that the bound metal ion gives rise to pseudocontact shifts that can be measured. This in turn requires that a substantial fraction of the protein is metal-bound, either because of a sufficiently large binding constant or because of a sufficiently large surplus of the metal ion. Preferably, the metal ion should be Ni^{2+} or another paramagnetic metal ion with a relatively fast electron relaxation rate to avoid excessive line broadening. Potential candidates among metal binding proteins are insulin, where the Zn^{2+} ion in the native Zn^{2+}-hexamer can be substituted by Ni^{2+} (*34*), human growth hormone (*35*), and α-synuclein (*36*).

ACKNOWLEDGMENT

We thank D. F. Hansen, S. M. Kristensen and M. A. S. Hass for helpful discussions, and C. Lauritzen, G. Petersen, and J. Pedersen, Unizyme A/S, for providing the Trx samples.

SUPPORTING INFORMATION AVAILABLE

Table containing the chemical shifts of the ^1H and ^{15}N nuclei in the metal-free and the Ni^{2+}-bound form of Trx. This material is available free of charge via the Internet at http://pubs.acs.org.

REFERENCES

1. Gochin, M. (1997) Nuclear Magnetic Resonance Studies of a Paramagnetic Metallo DNA Complex, *J. Am. Chem. Soc. 119*, 3377−3378.
2. Gochin, M. (2000) A High-Resolution Structure of a DNA-Chromomycin-Co(II) Complex Determined from Pseudocontact Shifts in Nuclear Magnetic Resonance, *Structure 8*, 441−452.
3. Tu, K., and Gochin, M. (1999) Structure Determination by Restrained Molecular Dynamics Using NMR Pseudocontact Shifts as Experimentally Determined Constraints, *J. Am. Chem. Soc. 121*, 9276−9285.
4. Allegrozzi, M., Bertini, I., Janik, M. B. L., Lee, Y. M., Lin, G. H., and Luchinat, C. (2000) Lanthanide-Induced Pseudocontact Shifts for Solution Structure Refinements of Macromolecules in Shells up to 40 Å from the Metal Ion, *J. Am. Chem. Soc. 122*, 4154−4161.
5. Arnesano, F., Banci, L., Bertini, I., and Felli, I. C. (1998) The Solution Structure of Oxidized Rat Microsomal Cytochrome b_5, *Biochemistry 37*, 173−184.
6. Baig, I., Bertini, I., Del Bianco, C., Gupta, Y. K., Lee, Y. M., Luchinat, C., and Quattrone, A. (2004) Paramagnetism-Based Refinement Strategy for the Solution Structure of Human α-Parvalbumin, *Biochemistry 43*, 5562−5573.
7. Bentrop, D., Bertini, I., Cremonini, M. A., Forsen, S., Luchinat, C., and Malmendal, A. (1997) Solution Structure of the Paramagnetic Complex of the N-Terminal Domain of Calmodulin with Two Ce^{3+} Ions by ^1H NMR, *Biochemistry 36*, 11605−11618.
8. Bertini, I., Janik, M. B. L., Lee, Y. M., Luchinat, C., and Rosato, A. (2001) Magnetic Susceptibility Tensor Anisotropies for a Lanthanide Ion Series in a Fixed Protein Matrix, *J. Am. Chem. Soc. 123*, 4181−4188.
9. Hus, J. C., Marion, D., and Blackledge, M. (2000) *De Novo* Determination of Protein Structure by NMR Using Orientational and Long-Range Order Restraints, *J. Mol. Biol. 298*, 927−936.
10. Donaldson, L. W., Skrynnikov, N. R., Choy, W. Y., Muhandiram, D. R., Sarkar, B., Forman-Kay, J. D., and Kay, L. E. (2001) Structural Characterization of Proteins with an Attached ATCUN Motif by Paramagnetic Relaxation Enhancement NMR Spectroscopy, *J. Am. Chem. Soc. 123*, 9843−9847.
11. Gaponenko, V., Dvoretsky, A., Walsby, C., Hoffman, B. M., and Rosevear, P. R. (2000) Calculation of *z*-Coordinates and Orientational Restraints Using a Metal Binding Tag, *Biochemistry 39*, 15217−15224.
12. Jensen, M. R., Lauritzen, C., Dahl, S. W., Pedersen, J., and Led, J. J. (2004) Binding Ability of a HHP-Tagged Protein Towards Ni^{2+} Studied by Paramagnetic NMR Relaxation: The Possibility of Obtaining Long-Range Structure Information, *J. Biomol. NMR 29*, 175−185.
13. Prudêncio, M., Rohovec, J., Peters, J. A., Tocheva, E., Boulanger, M. J., Murphy, M. E. P., Hupkes, H. J., Kosters, W., Impagliazzo, A., and Ubbink, M. (2004) A Caged Lanthanide Complex as a Paramagnetic Shift Agent for Protein NMR, *Chem.—Eur. J. 10*, 3252−3260.
14. Wöhnert, J., Franz, K. J., Nitz, M., Imperiali, B., and Schwalbe, H. (2003) Protein Alignment by a Coexpressed Lanthanide-Binding Tag for the Measurement of Residual Dipolar Couplings, *J. Am. Chem. Soc. 125*, 13338−13339.
15. Ikegami, T., Verdier, L., Sakhaii, P., Grimme, S., Pescatore, B., Saxena, K., Fiebig, K. M., and Griesinger, C. (2004) Novel Techniques for Weak Alignment of Proteins in Solution Using Chemical Tags Coordinating Lanthanide Ions, *J. Biomol. NMR 29*, 339−349.
16. Jensen, M. R., Petersen, G., Lauritzen, C., Pedersen, J., and Led, J. J. (2005) Metal Binding Sites in Proteins: Identification and Characterization by Paramagnetic NMR Relaxation, *Biochemistry 44*, 11014−11023.
17. Katti, S. K., Lemaster, D. M., and Eklund, H. (1990) Crystal Structure of Thioredoxin from *Escherichia coli* at 1.68 Å Resolution, *J. Mol. Biol. 212*, 167−184.
18. Jensen, M. R., Hansen, D. F., and Led, J. J. (2002) A General Method for Determining the Electron Self-Exchange Rates of Blue Copper Proteins by Longitudinal NMR Relaxation, *J. Am. Chem. Soc. 124*, 4093−4096.
19. Jeng, M. F., Campbell, A. P., Begley, T., Holmgren, A., Case, D. A., Wright, P. E., and Dyson, H. J. (1994) High-Resolution Solution Structures of Oxidized and Reduced *Escherichia coli* Thioredoxin, *Structure 2*, 853−868.
20. Dyson, H. J., Tennant, L. L., and Holmgren, A. (1991) Proton-Transfer Effects in the Active Site Region of *Escherichia coli* Thioredoxin Using Two-Dimensional ^1H NMR, *Biochemistry 30*, 4262−4268.
21. Donaire, A., Salgado, J., and Moratal, J. M. (1998) Determination of the Magnetic Axes of Cobalt(II) and Nickel(II) Azurins from ^1H NMR Data: Influence of the Metal and Axial Ligands on the Origin of Magnetic Anisotropy in Blue Copper Proteins, *Biochemistry 37*, 8659−8673.
22. Kurland, R. J., and McGarvey, B. R. (1970) Isotropic NMR Shifts in Transition Metal Complexes: The Calculation of the Fermi Contact and Pseudocontact Terms, *J. Magn. Reson. 2*, 286−301.
23. Bertini, I., Luchinat, C., and Turano, P. (2000) ^{15}N Chemical Shift Changes in Cytochrome b_5: Redox-Dependent vs. Guanidinium Chloride-Induced Changes, *J. Biol. Inorg. Chem. 5*, 761−764.
24. Boyd, J., Dobson, C. M., Morar, A. S., Williams, R. J. P., and Pielak, G. J. (1999) ^1H and ^{15}N Hyperfine Shifts of Cytochrome *c*, *J. Am. Chem. Soc. 121*, 9247−9248.

25. Jensen, M. R., Hansen, D. F., Ayna, U., Dagil, R., Hass, M. A. S., Christensen, H. E. M., and Led, J. J. (2006) On the Use of Pseudocontact Shifts in the Structure Determination of Metalloproteins, *Magn. Reson. Chem. 44*, 294−301.

26. Lehmann, T., Luchinat, C., and Piccioli, M. (2002) Redox-Related Chemical Shift Perturbations on Backbone Nuclei of High-Potential Iron−Sulfur Proteins, *Inorg. Chem. 41*, 1679−1683.

27. Tsan, P., Caffrey, M., Daku, M. L., Cusanovich, M., Marion, D., and Gans, P. (1999) Unusual Contact Shifts and Magnetic Tensor Orientation in *Rhodobacter capsulatus* Ferrocytochrome *c*′: NMR, Magnetic Susceptibility, and EPR Studies, *J. Am. Chem. Soc. 121*, 1795−1805.

28. de Dios, A. C., Pearson, J. G., and Oldfield, E. (1993) Secondary and Tertiary Structural Effects on Protein NMR Chemical Shifts—An Ab Initio Approach, *Science 260*, 1491−1496.

29. Neal, S., Nip, A. M., Zhang, H. Y., and Wishart, D. S. (2003) Rapid and Accurate Calculation of Protein ^{1}H, ^{13}C and ^{15}N Chemical Shifts, *J. Biomol. NMR 26*, 215−240.

30. Ma, L., Jørgensen, A.-M. M., Sørensen, G. O., Ulstrup, J., and Led, J. J. (2000) Elucidation of the Paramagnetic R_1 Relaxation of Heteronuclei and Protons in Cu(II) Plastocyanin from *Anabaena variabilis*, *J. Am. Chem. Soc. 122*, 9473−9485.

31. Schwieters, C. D., Kuszewski, J. J., Tjandra, N., and Clore, G. M. (2003) The Xplor-NIH NMR Molecular Structure Determination Package, *J. Magn. Reson. 160*, 65−73.

32. Banci, L., Bertini, I., Cavallaro, G., Giachetti, A., Luchinat, C., and Parigi, G. (2004) Paramagnetism-Based Restraints for Xplor-NIH, *J. Biomol. NMR 28*, 249−261.

33. Cornilescu, G., Marquardt, J. L., Ottiger, M., and Bax, A. (1998) Validation of Protein Structure from Anisotropic Carbonyl Chemical Shifts in a Dilute Liquid Crystalline Phase, *J. Am. Chem. Soc. 120*, 6836−6837.

34. Led, J. J., Grant, D. M., Horton, W. J., Sundby, F., and Vihelmsen, K. (1975) ^{13}C Magnetic Resonance Study of Structural and Dynamical Features in Carbamylated Insulins, *J. Am. Chem. Soc. 97*, 5997−6008.

35. Cunningham, B. C., Mulkerrin, M. G., and Wells, J. A. (1991) Dimerization of Human Growth Hormone by Zinc, *Science 253*, 545−548.

36. Rasia, R. M., Bertoncini, C. W., Marsh, D., Hoyer, W., Cherny, D., Zweckstetter, M., Griesinger, C., Jovin, T. M., and Fernandez, C. O. (2005) Structural Characterization of Copper(II) Binding to α-synuclein: Insights into the Bioinorganic Chemistry of Parkinson's Disease, *Proc. Natl. Acad. Sci. U.S.A. 102*, 4294−4299.

BI0604431